

# Conditions for static bubbles in visco-plastic fluids

Neville Dubash

*Department of Mathematics, Imperial College,*

*180 Queen's Gate, London, UK, SW7 2BZ\**

Ian Frigaard

*Department of Mathematics and Department of Mechanical Engineering,*

*University of British Columbia, 2324 Main Mall,*

*Vancouver, BC, Canada, V6T 1Z4.†*

(Dated: January 29, 2004)

# Abstract

We consider the propagation of a gas bubble in a cylindrical column filled with a visco-plastic fluid. Because of the yield stress of the fluid, it is possible that a bubble will remain trapped in the fluid indefinitely. We investigate this case of slow moving or near-stationary bubbles.

Using the Herschel-Bulkley constitutive equation to model our visco-plastic fluid, Prager's two variational principles are adapted to our problem. From these two principles we develop two stopping conditions, i.e. for a given bubble we can calculate a critical Bingham number above which the bubble will not move. The first condition is for axisymmetric bubbles and is dependent on the bubble length as well as the general shape of the bubble. The second stopping condition is essentially a comparison principle. It allows us to use solutions of simpler problems to calculate additional stopping conditions. We also develop a condition for bubble propagation. Finally, we illustrate the general stopping conditions by application to specific bubble shapes.

PACS numbers: 47.15.Gf, 47.50.+d, 47.55.Dz, 83.60.La

---

\*Electronic address: [neville.dubash@imperial.ac.uk](mailto:neville.dubash@imperial.ac.uk)

†Electronic address: [frigaard@math.ubc.ca](mailto:frigaard@math.ubc.ca)

## I. INTRODUCTION

In this paper we examine the propagation of gas bubbles through a visco-plastic fluid. Visco-plastic fluids are fluids that can behave as both a viscous liquid and as a rigid solid. Which of these two states the material takes is determined by the stress applied to the material. That is, at low stress the material behaves as a solid, capable of rigid motion and rotation. However, when stresses exceed a certain threshold, called the yield stress, the material behaves as a nonlinearly viscous liquid. Because of the yield stress of the fluid, two interesting phenomena can occur. First, bubbles can become trapped in the fluid indefinitely. This occurs when the buoyancy of the bubble is insufficient to break the yield stress, i.e., when

$$\hat{\tau}_Y \gg [\hat{\rho}_\ell - \hat{\rho}_g^*] \hat{g} \hat{R},$$

where  $\hat{\tau}_Y$ ,  $\hat{\rho}_\ell$ ,  $\hat{\rho}_g^*$ ,  $\hat{g}$  &  $\hat{R}$  are respectively the yield stress, fluid density, reference gas density, gravitational acceleration, and reference bubble length-scale. Secondly, a variety of stationary bubble shapes can exist. For sufficiently small bubbles, surface tension will dominate yield stress and bubbles are predominantly spherical, but when

$$\hat{\tau}_Y \gg \frac{\hat{\xi}}{\hat{R}},$$

surface tension is not important in determining the shape of the bubble, ( $\hat{\xi}$  denotes the coefficient of surface tension). Indeed for a given yield stress the shape of static bubbles appears to be non-unique. In Fig. 1 we show a range of static bubble shapes. In this paper we are interested in the case of slow moving and stationary bubbles, and in providing general conditions under which a given bubble will either rise or remain trapped.

Common examples of fluids with a yield stress are mud, cement, lava, and paint. A range of specific fluids with a yield stress are considered in [1]. Common constitutive models are

the Bingham, Casson, and Herschel-Bulkley models, see e.g., [1, 2]. Yield stress phenomena also occur in many foams, slurries, suspensions, and polymer solutions, which are common industrial fluids. There are many processes where the generation and behaviour of bubbles play a significant role. In some situations bubbles are undesirable, and while it would be ideal if they could be eliminated, in practice this is very difficult. This provides the principal motivation for our study. Some specific examples of such processes are as follows.

1. When drilling an oil well, gas kicks can occur. Drilling mud is generally a visco-plastic fluid. A kick occurs when the pressure within the wellbore, (primarily hydrostatic pressure of the mud), is unexpectedly less than the pore pressure of gas in the surrounding rock formation. Gas from the formation flows into the wellbore and rises upwards in the well, see e.g., [3]. If uncontrolled, a gas kick can lead to a blowout at the surface, with possible loss of life, environmental damage, and significant costs for the operator. Certainly there have been a number of horrific incidents of this kind, e.g., the Piper-Alpha incident in the North Sea in 1988.

Gas rise velocity in visco-plastic media has thus been studied extensively in the oil industry, typically experimentally; see [3–5] as representative examples. In general these studies are focused at multiple bubbles propagating in moving duct flows, with the aim being to derive empirical correlations for the slip velocity that can be used in gas kick simulation and prediction.

2. Many processed foods, (e.g., ketchup, mayonnaise, peanut butter, chocolate), and cosmetic products, (e.g., hair gel, hand cream), exhibit a yield stress. Bubbles may be either unwanted or highly desirable, e.g., aerated chocolate has a different taste than solid chocolate; hair gel is sold by volume, (bubbles included).

3. In the manufacture and processing of energetic materials (such as solid rocket fuels, etc.), shock waves that occur in processing cause the compression of any bubbles in the fluid. It is believed that when the gas is rapidly compressed a high-temperature spot (hot spot) can develop which may heat the surrounding explosive material to the point of auto-ignition, [6]. In practice the energetic material behaves as a visco-plastic during processing.

Separately, bubbles and visco-plastic fluids have been studied quite extensively. For the former subject, we refer the reader to texts on bubble dynamics, such as [7, 8]. Variational principles for visco-plastic fluids were first derived by Prager [9], for a single Bingham fluid. These have been generalised to Herschel-Bulkley fluids and to a range of different situations in [10–13]. Generalisation to the flow of multiple visco-plastic fluids is presented in [14–16]. We will extend from this work in deriving our variational principles. The other aspect of our results is the stopping criteria, or critical Bingham numbers, above which a bubble will not move. Obviously such criteria are present in simple analytical solutions, for example, a Poiseuille flow of a visco-plastic fluid only flows when a critical pressure gradient is exceeded. The first extensive study of this phenomena, and indeed of the shape of yield surfaces, is in the sequence of papers by Mosolov and Miasnikov, [17–19]. General results of this nature are also derived by Duvaut and Lions, [20], and the decay of transient solutions to zero in a finite time, if the critical Bingham number is exceeded, was demonstrated in [21].

The problem of the propagation of a single bubble in a visco-plastic fluid has yet to receive much attention. The special case of spherical bubbles has been examined in two papers [22, 23]. In Bhavaraju et al. [22], the authors examine the flow of a single spherical bubble in a Bingham fluid. They consider small Bingham numbers  $B$ , as a perturbation from the Newtonian solution for flow around a spherical bubble and obtain a first order

correction. However, their solution is only valid away from the equator of the bubble, and since  $B \ll 1$  is required, (so that there is continuity to the Newtonian solution as  $B \rightarrow 0$ ), the case of stationary bubbles is not considered. In [23] the authors show that spherical bubbles that are initially trapped in a Bingham fluid can be made to rise by applying an oscillating external pressure to the liquid. They use perturbation methods to derive an analytic solution that consists of a flow due to the pulsation and a flow due to the bubble rising under gravity. They have also conducted experiments that illustrate the phenomenon and that support their analytic results.

A related problem that has received more attention is the problem of slow flow past a solid sphere in visco-plastic fluids. Beris et al. [24], examine the fall of a sphere due to gravity in an infinite Bingham fluid. Using a finite element numerical simulation they obtain the flow field and the yield surfaces in the flow. Using asymptotic methods, they also obtain the critical Bingham number at which the sphere becomes static, and expressions for the drag coefficient. There have been extensions of this work to spheres falling in a tube, [25], attempts at experimental verification, [26], and further studies to extend the expressions for the drag coefficient, [27, 28]. Further work has addressed stick-slip boundary conditions on the sphere, [29], and attempted to experimentally determine the drag coefficient for other shapes, (such as discs, cylinders, cubes, and cones), see [30].

There is a good level of agreement amongst the studies on falling spheres, certainly beyond the qualitative level. However, both computational studies and experimental studies present some difficulties. For the computational studies, use of viscosity regularisation techniques, e.g., [25], can be problematic both for determining the critical  $B$  at which a visco-plastic stops flowing and for predicting the shape of the yield surface. Having said this, the results in [25], on the critical yield limit, appear to approach those of [24] smoothly for large tubes.

Experimentally, problems with repeatability and relaxation time have to be addressed with many laboratory fluids, see e.g., [31] for a discussion of some of the practical problems. Another issue with propagating bubbles, (e.g., through a Carbopol solution), is to use an appropriate rheological model, i.e., the Bingham model may be easiest from an analytical perspective, but does not model such experimental fluids well.

Other than the above studies, determination of yield limits in multi-fluid visco-plastic flows has been studied in [32, 33], in the context of axial exchange flows related to oilfield plug-cementing. There are also various papers that address multi-fluid and displacement flows of visco-plastic fluids in a range of contexts. For example, Alexandrou & Entov have considered a fingering bubble displacement along a Hele-Shaw cell, [34]. There are also related studies of displacement flows of visco-plastic fluids along long ducts, e.g., [14, 35]. Finally, Li and Renardy have numerically examined deformations of a viscous fluid drop in a Bingham fluid [36].

A brief outline of our paper is as follows. In section II we describe the physical problem and our mathematical model. In section III we present two variational results: a variational inequality that leads to a rate of strain minimization, and a stress maximization result. In section IV we use our variational results to obtain stopping conditions, under which a bubble will not move. The first condition is a result that applies to axisymmetric bubbles of arbitrary shape. The second condition allows us to use existing solutions of simpler problems to obtain extra stopping conditions. In section V we take our general stopping conditions and apply them to some specific bubble shapes. We close with a discussion in section VI.

## II. MATHEMATICAL FORMULATION

### A. Physical Setup

We consider the flow (or lack thereof) of a single gas bubble in a cylindrical column filled with a visco-plastic fluid, see Fig 2. Our domain is divided into two connected regions:  $\Omega$ , comprising the liquid region, and  $\Omega_b$ , comprising the gas domain (i.e., the bubble). The boundary of  $\Omega$ , consisting of both the cylinder walls and the bubble surface, will be referred to as  $\partial\Omega$ . The bubble surface on its own will be referred to as  $\partial\Omega_b$ , and the walls of the cylinder on their own will be referred to as  $\partial\Omega_w$  or simply as the ‘‘cylinder walls’’. Quantities denoted with a hat ‘‘ $\hat{\cdot}$ ’’ are dimensional while quantities without a hat are dimensionless. Where required, subscripts  $\ell$  &  $g$  denote parameters or variables, for liquid and gas, respectively. We also adopt the Einstein summation convention for coordinate indices.

Densities of liquid and gas phases are denoted  $\hat{\rho}_\ell$  and  $\hat{\rho}_g$ , respectively. The liquid, being visco-plastic, is modelled as an incompressible Herschel-Bulkley fluid and is characterised by its yield stress  $\hat{\tau}_Y$ , consistency  $\hat{\kappa}$ , and power-law index  $n$ . The gas is a compressible Newtonian fluid, with viscosity  $\hat{\mu}$ . Although compressible, we examine the case when the bubble does not move very fast, nor very far. It is assumed that a volume  $\hat{V}_b$  of gas has been injected, at a given pressure. The density of the gas at this pressure is denoted  $\hat{\rho}_g^*$ .

We define the dimensionless length, velocity, time, and pressure ( $x_i$ ,  $u_i$ ,  $t$ , and  $p$  respectively) by

$$\begin{aligned} \hat{x}_i &= \hat{R}x_i, & \hat{u}_i &= \hat{U}u_i, \\ \hat{t} &= \frac{\hat{R}}{\hat{U}}t, & \hat{p} &= \hat{\rho}_\ell \hat{g} \hat{R} p. \end{aligned}$$

In the above we have chosen the effective bubble radius,  $\hat{R} = \sqrt[3]{\frac{3}{4\pi}\hat{V}_b}$ , as the length scale.

Our velocity scale  $\hat{U}$  approximates the balance between viscous and buoyancy forces, i.e.,

$$\hat{U} \equiv \left( \frac{\hat{\rho}_\ell \hat{g} \hat{R}^{n+1}}{\hat{\kappa}} \right)^{\frac{1}{n}} \approx \left( \frac{[\hat{\rho}_\ell - \hat{\rho}_g^*] \hat{g} \hat{R}^{n+1}}{\hat{\kappa}} \right)^{\frac{1}{n}}, \quad (1)$$

note that  $\hat{\rho}_g^*/\hat{\rho}_\ell \ll 1$ , and the above scalings preempts our later model reduction. The pressure scale is simply the static pressure scale in the liquid, over the length scale of the bubble. All viscous stresses in gas and liquid are scaled with  $\hat{\kappa}(\hat{U}/\hat{R})^n$ .

The non-dimensional equations of motion in the fluid region  $\Omega$ , are

$$Fr^2 \frac{Du_i}{Dt} = -\frac{\partial p}{\partial x_i} - \delta_{i3} + \frac{\partial \tau_{ij}(\mathbf{u})}{\partial x_j}, \quad (2)$$

$$\frac{\partial u_i}{\partial x_i} = 0, \quad (3)$$

and in the bubble  $\Omega_b$ , we have

$$\epsilon \rho_g Fr^2 \frac{Du_i}{Dt} = -\frac{\partial p}{\partial x_i} - \epsilon \rho_g \delta_{i3} + \delta \frac{\partial \dot{\gamma}_{ij}(\mathbf{u})}{\partial x_j}, \quad (4)$$

$$\frac{\partial \rho_g}{\partial t} + \frac{\partial}{\partial x_i}(\rho_g u_i) = 0, \quad (5)$$

where  $\delta_{ij}$  is the Kronecker delta and we have taken the third basis vector to be pointing upwards, and  $D/Dt = \partial/\partial t + u_i \partial/\partial x_i$ . The dimensionless parameters above are

$$Fr = \frac{\hat{U}}{\sqrt{\hat{g} \hat{R}}}, \quad \epsilon = \frac{\hat{\rho}_g^*}{\hat{\rho}_\ell}, \quad \delta = \frac{\hat{\mu}_g \hat{R}^{n-1}}{\hat{\kappa} \hat{U}^{n-1}}, \quad (6)$$

denoting the Froude number, density ratio, and effective viscosity ratio respectively.

The gas density is simply  $\rho_g = \hat{\rho}_g/\hat{\rho}_g^*$ . The deviatoric stress tensor in the liquid is denoted  $\tau_{ij}(\mathbf{u})$ , and the rate of strain tensor  $\dot{\gamma}_{ij}(\mathbf{u})$ , is defined by

$$\dot{\gamma}_{ij}(\mathbf{u}) = \frac{\partial u_i}{\partial x_j} + \frac{\partial u_j}{\partial x_i}.$$

In the liquid the following constitutive equations for a Herschel-Bulkley fluid are satisfied:

$$\dot{\gamma}_{ij}(\mathbf{u}) = 0 \quad \text{if } \boldsymbol{\tau}(\mathbf{u}) \leq B, \quad (7)$$

$$\tau_{ij}(\mathbf{u}) = \left( \dot{\boldsymbol{\gamma}}(\mathbf{u})^{n-1} + \frac{B}{\dot{\boldsymbol{\gamma}}(\mathbf{u})} \right) \dot{\gamma}_{ij}(\mathbf{u}) \quad \text{if } \boldsymbol{\tau}(\mathbf{u}) > B, \quad (8)$$

where

$$B = \frac{\hat{\tau}_Y \hat{R}^n}{\hat{\kappa} \hat{U}^n} = \frac{\hat{\tau}_Y}{\hat{\rho}_\ell \hat{g} \hat{R}} \approx \frac{\hat{\tau}_Y}{[\hat{\rho}_\ell - \hat{\rho}_g^*] \hat{g} \hat{R}} \quad (9)$$

is the Bingham number. The second invariants of the dimensionless rate of strain and deviatoric stress tensors are

$$\dot{\gamma}(\mathbf{u}) = \sqrt{\frac{1}{2} \dot{\gamma}_{ij}(\mathbf{u}) \dot{\gamma}_{ij}(\mathbf{u})}, \quad \text{and} \quad \boldsymbol{\tau}(\mathbf{u}) = \sqrt{\frac{1}{2} \tau_{ij}(\mathbf{u}) \tau_{ij}(\mathbf{u})}.$$

Finally, the bubble interface,  $\partial\Omega_b$ , whose location is denoted by  $F(\mathbf{x}, t) = 0$ , evolves according to the kinematic condition

$$\frac{\partial F}{\partial t} + u_i \frac{\partial F}{\partial x_i} = 0. \quad (10)$$

## B. Simplified Dimensionless Model

Before discussing boundary and interfacial conditions, we simplify our model. First, for slow flows we can ignore the inertial terms, which scale as  $\sim u_i^2$ , whereas the remaining terms scale as  $\sim u_i$ . Since we are interested in the phenomena of stopped bubbles and “nearly” stopped bubbles, the inertial terms can be considered to be an order of magnitude smaller than the other terms in this limit. Second, we have in mind a typical combination of an aqueous visco-plastic polymer solution (e.g. Carbopol), and an air bubble, for which  $\delta \sim 10^{-6}$  and  $\epsilon \sim 10^{-3}$ . Thus, as a first approximation, we also ignore the terms containing  $\delta$  and  $\epsilon$ . Equations (2) and (4) become

$$\text{liquid:} \quad 0 = -\frac{\partial p}{\partial x_i} - \delta_{i3} + \frac{\partial \tau_{ij}(\mathbf{u})}{\partial x_j}, \quad (11)$$

$$\text{gas:} \quad 0 = -\frac{\partial p}{\partial x_i} \quad (12)$$

respectively.

In the liquid we still have (3). Equation (12) implies that the pressure in the bubble is constant, ( $p = p(t)$ ). The dimensional version of equation (5) can be written as

$$\begin{aligned}
\frac{\partial \hat{\rho}_g}{\partial \hat{t}} + \hat{u}_i \frac{\partial \hat{\rho}_g}{\partial \hat{x}_i} + \hat{\rho}_g \frac{\partial \hat{u}_i}{\partial \hat{x}_i} &= 0 \\
\frac{1}{\hat{\rho}_g} \frac{\partial \hat{\rho}_g}{\partial \hat{p}} \left( \frac{\partial \hat{p}}{\partial \hat{t}} + \hat{u}_i \frac{\partial \hat{p}}{\partial \hat{x}_i} \right) + \frac{\partial \hat{u}_i}{\partial \hat{x}_i} &= 0 \\
\frac{1}{\hat{\rho}_g} \frac{\partial \hat{\rho}_g}{\partial \hat{p}} \frac{\partial \hat{p}}{\partial \hat{t}} + \frac{\partial \hat{u}_i}{\partial \hat{x}_i} &= 0 \\
\frac{1}{\hat{\rho}_g \hat{c}_g^2} \frac{\partial \hat{p}}{\partial \hat{t}} + \frac{\partial \hat{u}_i}{\partial \hat{x}_i} &= 0,
\end{aligned} \tag{13}$$

where  $\hat{c}_g = \sqrt{\partial \hat{p} / \partial \hat{\rho}_g}$ , is the speed of sound in the gas, and we have used (12). Now the main change in the bubble pressure is due to the reduction in static pressure of the liquid as the bubble slowly rises; when  $\hat{p}$  changes like  $\hat{\rho}_\ell \hat{g} \hat{U}$ . Examining the relative sizes of the two terms in (13) we have  $\partial \hat{u}_i / \partial \hat{x}_i \sim \hat{U} / \hat{R}$  and  $\frac{1}{\hat{\rho}_g \hat{c}_g^2} \frac{\partial \hat{p}}{\partial \hat{t}} \sim \hat{g} \hat{U} / \epsilon \hat{c}_g^2$ . So

$$\frac{\frac{1}{\hat{\rho}_g \hat{c}_g^2} \frac{\partial \hat{p}}{\partial \hat{t}}}{\frac{\partial \hat{u}_i}{\partial \hat{x}_i}} \sim \frac{\hat{g} \hat{R}}{\epsilon \hat{c}_g^2} \approx \frac{(10)(10^{-2})}{(10^{-3})(10^5)} = 10^{-3},$$

for bubbles of radii  $\lesssim 1$ cm. Thus we make the approximation of incompressibility also for the bubble:

$$\frac{\partial u_i}{\partial x_i} = 0. \tag{14}$$

### 1. Boundary and interfacial conditions

On the walls and base of the liquid column we have the no-slip condition:

$$u_i = 0, \quad \text{on } \partial\Omega_w. \tag{15}$$

At the top of the cylinder we have a free surface. A realistic set of boundary conditions here would be to impose the condition of zero traction and to allow the free surface to rise vertically in order to take account of any expansion of the bubble. However, we have shown

above that the rate of increase in volume, due to bubble rise and expansion, is relatively small in the slow flow limit, so that (14) is a reasonable approximation. Due to the approximation (14), there is no net rise in the free surface. Hence for simplicity, we also impose (15) at the top of the column. Alternatively we could consider bubble rise in a sealed column, i.e., not allowing any expansion.

On the bubble surface, the velocity and the tangential components of the traction must be continuous across the bubble surface. However, in the limit  $\delta \rightarrow 0$ , that we consider, there is no traction from within the bubble. Hence, we have:

$$u_{\ell,i} - u_{g,i} = 0 \quad \text{across } \partial\Omega_b, \quad (16)$$

$$\tau_{n_b t_1} = 0, \quad (17)$$

$$\tau_{n_b t_2} = 0, \quad (18)$$

where  $\mathbf{n}_b$  is the outward unit normal of the bubble (i.e., pointing into the fluid region), and  $\mathbf{t}_1$  and  $\mathbf{t}_2$  are two independent unit vectors tangent to the surface of the bubble. The jump in the normal component of the traction must be balanced by surface tension. Thus,

$$-p_\ell + p_g + \tau_{n_b n_b} = \beta \left( \frac{1}{R_1} + \frac{1}{R_2} \right) \quad (19)$$

on  $\partial\Omega_b$ , where

$$\beta = \frac{\hat{\xi}}{\hat{\rho}_\ell \hat{g} \hat{R}^2} \quad (20)$$

is the dimensionless surface tension coefficient, and  $R_1 = \hat{R}_1/\hat{R}$  and  $R_2 = \hat{R}_2/\hat{R}$  are the dimensionless radii of curvature.

### III. VARIATIONAL PRINCIPLES

We see that in the classical formulation, (3), (7), (8), (10), (11), (12), (14), and (15)–(19), time dependency enters the problem only through (10). That is, at each time we have a

Stokes problem to solve for the particular interface configuration; the interface then advances through the kinematic condition (10). Hence, here we look solely at the Stokes problem (3), (7), (8), (11), (12), (14), (15)–(19). Our objective is first to derive two variational principles for this problem and then later to use these to derive conditions under which  $\mathbf{u} = 0$ , is the sole solution. For such conditions the bubble cannot move. The principles that we derive are variations of those first derived by Prager [9] for slow Bingham fluid flows.

### A. Variational inequality (rate of strain minimization)

From (3), (7), (8), (11), (12), (14), (15)–(19), it can be shown that the solution,  $\mathbf{u} \in \bar{V}$ , satisfies

$$a(\mathbf{u}, \mathbf{v} - \mathbf{u}) + j(\mathbf{v}) - j(\mathbf{u}) \geq L(\mathbf{v} - \mathbf{u}) \quad \forall \mathbf{v} \in \bar{V} \quad (21)$$

where

$$a(\mathbf{u}, \mathbf{v}) = \frac{1}{2} \int_{\Omega} \dot{\gamma}(\mathbf{u})^{n-1} \dot{\gamma}_{ij}(\mathbf{u}) \dot{\gamma}_{ij}(\mathbf{v}) d\Omega, \quad (22)$$

$$j(\mathbf{u}) = B \int_{\Omega} \dot{\gamma}(\mathbf{u}) d\Omega, \quad \text{and} \quad (23)$$

$$L(\mathbf{u}) = - \int_{\Omega} u_3 d\Omega - \int_{\partial\Omega_b} \beta \left( \frac{1}{R_1} + \frac{1}{R_2} \right) u_i n_{b,i} ds. \quad (24)$$

The steps to derive (21) are straightforward and we refer to [12] for detailed derivation of a similar inequality with slightly different boundary conditions. The space of functions we consider, denoted  $\bar{V}$ , is the closure of the space  $V$  with respect to the  $[W^{1+n}(\Omega)]^3$  norm, i.e., for  $\mathbf{v} = (v_1, v_2, v_3) \in \bar{V}$ , we define  $\|\mathbf{v}\|$  by:

$$\|\mathbf{v}\| = \left[ \int_{\Omega} \sum_i |v_i|^{n+1} + \sum_{i,j} \left| \frac{\partial v_i}{\partial x_j} \right|^{n+1} d\Omega \right]^{1/(n+1)}. \quad (25)$$

The space  $V$ , is the space of all vector-valued functions  $\mathbf{v} = (v_1, v_2, v_3)$ , such that

$$v_i \in C^\infty(\Omega), \quad (26)$$

$$\frac{\partial v_i}{\partial x_i} = 0 \quad \text{in } \Omega, \text{ and} \quad (27)$$

$$v_i = 0 \quad \text{on } \partial\Omega_w. \quad (28)$$

**Remarks:**

1. Note that  $a(\cdot, \cdot)$  is linear in its second argument,  $L(\cdot)$  is linear, but  $j(\cdot)$  is non-linear. Sometimes  $a(\cdot, \cdot)$  is referred to as the viscous dissipation rate and  $j(\cdot)$  is called the yield stress dissipation rate.
2. In [12], Huilgol lists a number of generic boundary condition combinations for which a variational formulation analogous to (21) can be found. Our problem does not fall into one of these classes.
3. In the sequel we shall assume the existence of a unique solution to (21). Assuming sufficient regularity on the bubble shape, this does not appear to be too difficult to prove, but adds little to the results in the paper.

An alternate formulation to (21), that we shall use later, is as a pure minimization problem. Consider the convex functional  $H(\mathbf{u})$ :

$$H(\mathbf{u}) = \frac{1}{n+1}a(\mathbf{u}, \mathbf{u}) = \frac{1}{2(n+1)} \int_{\Omega} \dot{\boldsymbol{\gamma}}(\mathbf{u})^{n-1} \dot{\gamma}_{ij}(\mathbf{u}) \dot{\gamma}_{ij}(\mathbf{u}) d\Omega. \quad (29)$$

The Gâteaux derivative of  $H$  in the direction  $\mathbf{v}$  is

$$\delta H(\mathbf{u}; \mathbf{v}) = \frac{1}{2} \int_{\Omega} \dot{\boldsymbol{\gamma}}(\mathbf{u})^{n-1} \dot{\gamma}_{ij}(\mathbf{u}) \dot{\gamma}_{ij}(\mathbf{v}) d\Omega = a(\mathbf{u}, \mathbf{v}). \quad (30)$$

Since  $H$  is Gâteaux differentiable and convex we have that

$$\frac{1}{n+1}a(\mathbf{v}, \mathbf{v}) - \frac{1}{n+1}a(\mathbf{u}, \mathbf{u}) = H(\mathbf{v}) - H(\mathbf{u}) \geq \delta H(\mathbf{u}; \mathbf{v} - \mathbf{u}) = a(\mathbf{u}, \mathbf{v} - \mathbf{u}), \quad (31)$$

(see e.g., Proposition 2.2 of chapter 5 in [21]). Substituting (31) into (21) and recalling that  $L(\cdot)$  is linear we obtain, for  $\mathbf{v} \in \bar{V}$ ,

$$\begin{aligned} \frac{1}{n+1}a(\mathbf{v}, \mathbf{v}) - \frac{1}{n+1}a(\mathbf{u}, \mathbf{u}) + j(\mathbf{v}) - j(\mathbf{u}) &\geq L(\mathbf{v}) - L(\mathbf{u}) \\ \Rightarrow \frac{1}{n+1}a(\mathbf{v}, \mathbf{v}) + j(\mathbf{v}) - L(\mathbf{v}) &\geq \frac{1}{n+1}a(\mathbf{u}, \mathbf{u}) + j(\mathbf{u}) - L(\mathbf{u}). \end{aligned} \quad (32)$$

So the true velocity field,  $\mathbf{u}$ , distinguishes itself from all other velocity fields,  $\mathbf{v} \in \bar{V}$ , in that  $\mathbf{u}$  minimizes the functional

$$J(\mathbf{v}) \equiv \frac{1}{n+1}a(\mathbf{v}, \mathbf{v}) + j(\mathbf{v}) - L(\mathbf{v}) \quad (33)$$

over the functional space  $\bar{V}$ .

Furthermore, if in equation (21) we let  $\mathbf{v} = 2\mathbf{u}$  and  $\mathbf{v} = 0$ , then we see that

$$a(\mathbf{u}, \mathbf{u}) + j(\mathbf{u}) = L(\mathbf{u}). \quad (34)$$

Thus, from (34), we find the value of the functional  $J$  at the minimum:

$$J(\mathbf{u}) = -\frac{n}{n+1}a(\mathbf{u}, \mathbf{u}). \quad (35)$$

We shall use this minimization formulation later.

## B. Stress maximization principle

Our second variational principle is related to the stress maximization principle of Prager, [9]. It is based on the following fundamental result.

**Theorem 1:** If  $\mathbf{u}$  is the solution of the classical problem, then the true stress field,  $\tau_{ij}$ , maximizes the functional

$$F(\tilde{\tau}_{ij}) = -\frac{1}{2^{\frac{1}{n}+1}} \frac{n}{n+1} \int_{\Omega} (|\tilde{\boldsymbol{\tau}} - B| + \tilde{\boldsymbol{\tau}} - B)^{\frac{1}{n}+1} d\Omega + \int_{\Omega} \frac{1}{2} \tilde{\tau}_{ij} \dot{\gamma}_{ij}(\mathbf{u}) d\Omega. \quad (36)$$

over the set of all symmetric tensors  $\tilde{\tau}_{ij}$ .

**Remarks:**

1. The proof follows almost exactly that of Theorem 1 in Frigaard, et al. [15], and is not repeated. It should be noted that to prove theorem 1 does not require any further condition beyond symmetry of  $\tilde{\tau}_{ij}$ , although it is required that (36) is well-defined and that  $\tau_{ij}$  &  $\dot{\gamma}_{ij}(\mathbf{u})$  satisfy the constitutive laws, (see [15]).
2. Although not proven, Theorem 1 probably also holds for a weak solution  $\mathbf{u} \in \bar{V}$  that is the minimiser of (33), and then we may take symmetric tensors  $\tilde{\tau}_{ij} \in L^{1+1/n}(\Omega)$ . However, we proceed purely formally below.

Consider a symmetric stress field  $\tilde{\sigma}_{ij}$ . We say that the stress field  $\tilde{\sigma}_{ij} = -\tilde{p}\delta_{ij} + \tilde{\tau}_{ij}$ , or equivalently the pair  $(\tilde{p}, \tilde{\tau}_{ij})$ , is admissible if

$$0 = -\frac{\partial \tilde{p}}{\partial x_i} + \frac{\partial \tilde{\tau}_{ij}}{\partial x_j} - \delta_{i3} \quad \text{in } \Omega, \quad (37)$$

$$\tilde{\tau}_{n_b t_1} = 0 \quad \text{on } \partial\Omega_b, \quad (38)$$

$$\tilde{\tau}_{n_b t_2} = 0 \quad \text{on } \partial\Omega_b, \quad (39)$$

$$-\tilde{p} + \tilde{\tau}_{n_b n_b} = -p_g + \beta \left( \frac{1}{R_1} + \frac{1}{R_2} \right) \quad \text{on } \partial\Omega_b, \quad (40)$$

and denote by  $T$  the set of admissible symmetric stress tensors. Later we shall also consider *weakly admissible* stress tensors, in which we shall relax the requirements (38-40).

Using the incompressibility of  $\mathbf{u}$ , symmetry of  $\tilde{\tau}_{ij}$ , and the divergence theorem, we have

$$\frac{1}{2} \int_{\Omega} \tilde{\tau}_{ij} \dot{\gamma}_{ij}(\mathbf{u}) \, d\Omega = - \int_{\Omega} u_3 \, d\Omega - \int_{\partial\Omega_b} (-\tilde{p}\delta_{ij} + \tilde{\tau}_{ij}) u_i n_{b,j} \, ds, \quad (41)$$

where  $\mathbf{n}_b$  is the outward unit normal of the bubble. We resolve the stress into normal and tangential components, to give

$$\frac{1}{2} \int_{\Omega} \tilde{\tau}_{ij} \dot{\gamma}_{ij}(\mathbf{u}) \, d\Omega = - \int_{\Omega} u_3 \, d\Omega - \int_{\partial\Omega_b} [(-\tilde{p} + \tilde{\tau}_{n_b n_b}) u_{n_b} + \tilde{\tau}_{t_1 n_b} u_{t_1} + \tilde{\tau}_{t_2 n_b} u_{t_2}], \quad (42)$$

where  $\mathbf{t}_1$  &  $\mathbf{t}_2$  are two orthonormal tangent vectors to  $\mathbf{n}_b$ . The above is true for any weakly admissible stress field. For an admissible stress field, conditions (38-40) imply that:

$$\frac{1}{2} \int_{\Omega} \tilde{\tau}_{ij} \dot{\gamma}_{ij}(\mathbf{u}) d\Omega = - \int_{\Omega} u_3 d\Omega - \int_{\partial\Omega_b} \beta \left( \frac{1}{R_1} + \frac{1}{R_2} \right) u_{n_b} ds. \quad (43)$$

Therefore, for any admissible stress field we can write the functional (36) as

$$F(\tilde{\tau}_{ij}) = G(\tilde{\tau}_{ij}) - \int_{\Omega} u_3 d\Omega - \int_{\partial\Omega_b} \beta \left( \frac{1}{R_1} + \frac{1}{R_2} \right) u_{n_b} ds, \quad (44)$$

where

$$G(\tilde{\tau}_{ij}) = - \frac{1}{2^{\frac{1}{n}+1}} \frac{n}{n+1} \int_{\Omega} (|\tilde{\boldsymbol{\tau}} - B| + \tilde{\boldsymbol{\tau}} - B)^{\frac{1}{n}+1} d\Omega. \quad (45)$$

The last two terms on the right-hand side of (44) are constant for a given bubble, only the first term depends on  $\tilde{\tau}_{ij}$ . Thus, we have:

**Theorem 2:** The true stress field,  $\tau_{ij}$ , maximizes the functional  $G(\tilde{\tau}_{ij})$  over all admissible  $(\tilde{p}, \tilde{\tau}_{ij})$ .

It can be seen that the only contribution to (45) come from areas in the fluid where the stress is above the yield stress. Hence the bubble travels in such a way as to minimize the stress in the yielded regions.

#### IV. GENERAL CONDITIONS FOR STATIC AND MOVING BUBBLES

We are primarily concerned with stopped bubbles and with conditions which determine whether a given bubble will propagate in the visco-plastic fluid or will become trapped. First we show that there will in general be a well-defined critical Bingham number above which a bubble cannot flow.

### A. Critical Bingham numbers from rate of strain minimisation

From the equality (34) and because  $a(\mathbf{u}, \mathbf{u}) \geq 0$ , we have that  $j(\mathbf{u}) \leq L(\mathbf{u})$ , for the solution  $\mathbf{u}$ . Assuming that  $\mathbf{u} \neq 0$ , we may write

$$\begin{aligned} B \int_{\Omega} \dot{\gamma}(\mathbf{u}) d\Omega &\leq - \int_{\Omega} u_3 d\Omega - \int_{\partial\Omega_b} \beta \left( \frac{1}{R_1} + \frac{1}{R_2} \right) u_i n_{b,i} ds, \\ B &\leq - \frac{\int_{\Omega} u_3 d\Omega}{\int_{\Omega} \dot{\gamma}(\mathbf{u}) d\Omega} - \frac{\int_{\partial\Omega_b} \beta \left( \frac{1}{R_1} + \frac{1}{R_2} \right) u_i n_{b,i} ds}{\int_{\Omega} \dot{\gamma}(\mathbf{u}) d\Omega}. \end{aligned} \quad (46)$$

Or equivalently, for

$$B \geq B_c \equiv \sup_{\forall \mathbf{v} \in \bar{V}, \mathbf{v} \neq 0} \left\{ - \frac{\int_{\Omega} v_3 d\Omega}{\int_{\Omega} \dot{\gamma}(\mathbf{v}) d\Omega} - \frac{\int_{\partial\Omega_b} \beta \left( \frac{1}{R_1} + \frac{1}{R_2} \right) v_i n_{b,i} ds}{\int_{\Omega} \dot{\gamma}(\mathbf{v}) d\Omega} \right\} \quad (47)$$

the only possible solution is one with  $\mathbf{u} = 0$  identically over  $\Omega$ . Thus, for a given shape of bubble, (47) defines a critical Bingham number  $B_c$  above which the bubble will not move.

Condition (47) becomes a little clearer if we confine our attention to an axisymmetric bubble, moving at steady speed  $U_b$  in a cylindrical column of radius  $R_c$ ; see Fig. 3. The radius of the bubble at a height  $z$  is given by the function  $r = f(z)$ , with  $f(z) = 0$  for  $z \geq z_+$  and for  $z \leq z_-$ . In order for there to be steady propagation, the velocity must lie in the subset of  $\bar{V}$  for which

$$\mathbf{v} = U_b \mathbf{e}_z + \mathbf{v}', \quad (48)$$

where  $\mathbf{e}_z$  is the unit vector in the  $z$ -direction and where  $\mathbf{v}' \cdot \mathbf{n}_b = 0$ . We denote this space by  $\bar{V}'$ . In terms of  $(r, z)$ -coordinates, we can write

$$\mathbf{n}_b = \left( \frac{1}{[1 + (f'(z))^2]^{1/2}}, \frac{-f'(z)}{[1 + (f'(z))^2]^{1/2}} \right),$$

and using basic differential geometry results from, [37],

$$\left( \frac{1}{R_1} + \frac{1}{R_2} \right) = - \frac{f'' f - (f')^2 - 1}{f((f')^2 + 1)^{\frac{3}{2}}}.$$

Therefore, the surface tension integral in (47) is simply:

$$\int_{\partial\Omega_b} \beta \left( \frac{1}{R_1} + \frac{1}{R_2} \right) v_i n_{b,i} ds = \beta U_b \int_{\partial\Omega_b} \frac{f'(f''f - (f')^2 - 1)}{f((f')^2 + 1)^2} ds \quad (49)$$

From the condition of incompressibility, we have that

$$U_b V_b = - \int_{\Omega} v_3 d\Omega \quad (50)$$

where  $V_b = \frac{4}{3}\pi$  is the volume of the bubble. Consequently, we may write

$$\int_{\partial\Omega_b} \beta \left( \frac{1}{R_1} + \frac{1}{R_2} \right) v_i n_{b,i} ds = -\frac{\beta}{V_b} \left( \int_{\Omega} u_3 d\Omega \right) \int_{\partial\Omega_b} \frac{f'(f''f - (f')^2 - 1)}{f((f')^2 + 1)^2} ds \quad (51)$$

and for steadily moving axisymmetric bubbles, (47) becomes:

$$B \geq B_{c,a} \equiv \left( 1 - \frac{2\pi\beta}{V_b} \int_{z_-}^{z_+} \frac{f'(f''f - (f')^2 - 1)}{[(f')^2 + 1]^{\frac{3}{2}}} dz \right) \left( \sup_{\forall \mathbf{v} \in \bar{V}', \mathbf{v} \neq 0} \left\{ -\frac{\int_{\Omega} v_3 d\Omega}{\int_{\Omega} \dot{\gamma}(\mathbf{v}) d\Omega} \right\} \right) \quad (52)$$

### 1. Bubbles shapes that do not propagate

If  $U_b \geq 0$  then we see that the axisymmetric critical Bingham number will be negative provided that:

$$1 - \frac{2\pi\beta}{V_b} \int_{z_-}^{z_+} \frac{f'(f''f - (f')^2 - 1)}{[(f')^2 + 1]^{\frac{3}{2}}} dz \leq 0. \quad (53)$$

Since  $B > 0$  for a yield stress fluid, for any bubble shape satisfying (53) the bubble cannot move. Condition (53) will be satisfied for bubble shapes for which the integral

$$S = \int_{z_-}^{z_+} \frac{f'(f''f - (f')^2 - 1)}{[(f')^2 + 1]^{\frac{3}{2}}} dz \quad (54)$$

is sufficiently large. Alternatively, if  $S > 0$  in (54), then for sufficiently large surface tension term  $\beta$ , the bubble cannot move. This result holds for Newtonian fluids also.

It should be noted that mathematically it is straightforward to construct a shape for which  $S > 0$ . For any given bubble given shape, if  $S < 0$ , then reflecting the shape in a

horizontal plane would change the sign of the integral, resulting in a positive value. For a bubble with fore-aft symmetry,  $S = 0$ . In Fig. 4 we show two actual bubble profiles (bubble velocity is upwards) for which  $S$  has opposite sign.

$$2. \text{ Bounding } -\int_{\Omega} v_3 d\Omega / \int_{\Omega} \dot{\gamma}(\mathbf{v}) d\Omega$$

When (53) does not hold, we may still compute a critical Bingham number from (52), by determining an upper limit for

$$\sup_{\forall \mathbf{v} \in \bar{V}', \mathbf{v} \neq 0} \left\{ -\frac{\int_{\Omega} v_3 d\Omega}{\int_{\Omega} \dot{\gamma}(\mathbf{v}) d\Omega} \right\}. \quad (55)$$

To do this we consider the fluid domain  $\Omega$  divided into three regions: the fluid above  $z_+$ , the fluid below  $z_-$ , and the fluid between  $z_-$  and  $z_+$ .

For the fluid above  $z_+$

$$v_3 = \int_L^z \frac{\partial v_3}{\partial \tilde{z}}(x, y, \tilde{z}) d\tilde{z},$$

since  $v_3 = 0$  on the top wall of the cylinder (i.e., at  $z = L$ ). So for a horizontal cross section at height  $z > z_+$

$$\begin{aligned} \int_{x^2+y^2 \leq R_c^2} v_3 dx dy &= \int_{x,y} \left( \int_L^z \frac{\partial v_3}{\partial \tilde{z}}(x, y, \tilde{z}) d\tilde{z} \right) dx dy \\ &= \int_L^z \frac{\partial}{\partial \tilde{z}} \left( \int_{x^2+y^2 \leq R_c^2} v_3(x, y, \tilde{z}) dx dy \right) d\tilde{z} = 0, \end{aligned}$$

since the net flux across each plane above  $z_+$  is zero. Similarly, for any plane below  $z_-$ . Thus the only contribution to the numerator in (55) is from the fluid between  $z_+$  and  $z_-$ .

$$\int_{\Omega} v_3 d\Omega = \int_{z_-}^{z_+} \left( \int_{f(z)^2 \leq x^2+y^2 \leq R_c^2} v_3(x, y, z) dx dy \right) dz. \quad (56)$$

Let  $z_{\frac{1}{2}} = (z_+ + z_-)/2$  be the midpoint of the bubble length, and let  $\Omega_+$  be the region of  $\Omega$

above  $z_{\frac{1}{2}}$  and  $\Omega_-$  be the region of  $\Omega$  below  $z_{\frac{1}{2}}$ , then for  $z \geq z_{\frac{1}{2}}$  we have

$$\begin{aligned}
-\int_{f(z)^2 \leq x^2 + y^2 \leq R_c^2} v_3 \, dx \, dy &= -\int_{f(z)^2 \leq x^2 + y^2 \leq R_c^2} \left( \int_L^z \frac{\partial v_3}{\partial \tilde{z}}(x, y, \tilde{z}) \, d\tilde{z} \right) \, dx \, dy \\
&= \int_{f(z)^2 \leq x^2 + y^2 \leq R_c^2} \left( \int_z^{z+} \frac{\partial v_3}{\partial \tilde{z}}(x, y, \tilde{z}) \, d\tilde{z} \right) \, dx \, dy \\
&\leq \int_z^{z+} \left( \int_{f(\tilde{z})^2 \leq x^2 + y^2 \leq R_c^2} \left| \frac{\partial v_3}{\partial \tilde{z}}(x, y, \tilde{z}) \right| \, dx \, dy \right) \, d\tilde{z} \\
&\leq \frac{1}{\sqrt{2}} \int_{z_{\frac{1}{2}}}^{z+} \left( \int_{f(\tilde{z})^2 \leq x^2 + y^2 \leq R_c^2} \dot{\gamma}(\mathbf{v}(x, y, \tilde{z})) \, dx \, dy \right) \, d\tilde{z} \\
&= \frac{1}{\sqrt{2}} \int_{\Omega_+} \dot{\gamma}(\mathbf{v}) \, d\Omega.
\end{aligned}$$

Similarly for  $z < z_{\frac{1}{2}}$  we have

$$\int_{f(z)^2 \leq x^2 + y^2 \leq R_c^2} v_3 \, dx \, dy \leq \frac{1}{\sqrt{2}} \int_{\Omega_-} \dot{\gamma}(\mathbf{v}) \, d\Omega.$$

Hence from (56) we obtain

$$\begin{aligned}
\int_{\Omega} v_3 \, d\Omega &\leq \int_{z_-}^{z_{\frac{1}{2}}} \left( \frac{1}{\sqrt{2}} \int_{\Omega_-} \dot{\gamma}(\mathbf{v}) \, d\Omega \right) \, dz + \int_{z_{\frac{1}{2}}}^{z_+} \left( \frac{1}{\sqrt{2}} \int_{\Omega_+} \dot{\gamma}(\mathbf{v}) \, d\Omega \right) \, dz \\
&= \frac{1}{2\sqrt{2}} (z_+ - z_-) \int_{\Omega} \dot{\gamma}(\mathbf{v}) \, d\Omega.
\end{aligned} \tag{57}$$

Therefore, substituting into (52), we have the following upper bound for the critical Bingham number,  $B_{c,a}$ , for a steadily moving axisymmetric bubble:

$$B_{c,a} \leq \frac{1}{2\sqrt{2}} (z_+ - z_-) \left( 1 - \frac{2\pi\beta}{V_b} \int_{z_-}^{z_+} \frac{f'(f''f - (f')^2 - 1)}{((f')^2 + 1)^{\frac{3}{2}}} \, dz \right). \tag{58}$$

and we have the following general result.

**Theorem 3:** For an axisymmetric bubble propagating steadily at speed  $U_b$ , with profile  $r = f(z)$ , if

$$B > \frac{1}{2\sqrt{2}} (z_+ - z_-) \left( 1 - \frac{2\pi\beta}{V_b} \int_{z_-}^{z_+} \frac{f'(f''f - (f')^2 - 1)}{((f')^2 + 1)^{\frac{3}{2}}} \, dz \right) \tag{59}$$

then  $U_b = 0$ .

## B. Critical Bingham numbers from stress maximisation: a comparison principle

A second general principle that can be used for computing a critical Bingham number comes from Theorem 2. We note that the functional  $G(\tilde{\tau}_{ij})$  in (45) is negative. Indeed the integrand of  $G(\tilde{\tau}_{ij})$  is non-zero only at points in  $\Omega$  where the yield stress,  $B$ , is exceeded by  $\tilde{\tau}$ . The following result follows:

**Theorem 4:** If  $(\tilde{p}, \tilde{\tau}_{ij})$  is an admissible stress field and if

$$K_{\tilde{\tau}} = \sup_{\mathbf{x} \in \Omega} \tilde{\tau}(\mathbf{x}), \quad (60)$$

then the bubble does not move if  $B \geq K_{\tilde{\tau}}$ .

The proof is automatic, since if  $B \geq K_{\tilde{\tau}}$  then  $G(\tilde{\tau}_{ij}) = 0$  which implies  $G(\tau_{ij}) = 0$  for the true stress field. But we note that for the true stress field:

$$G(\tau_{ij}) = -\frac{n}{n+1}a(\mathbf{u}, \mathbf{u}),$$

and  $a(\mathbf{u}, \mathbf{u}) = 0 \implies \mathbf{u} = 0$ .

Theorem 4 above is essentially a comparison principle. If for a given problem we can find an admissible stress field then we can obtain a stopping criterion. Admissible stress fields can be obtained from the solutions of simpler problems, e.g., the solution of a problem with the same geometry but with a Newtonian fluid (or a Power Law fluid).

As a corollary to theorem 4, we note that the stopping condition for a Herschel-Bulkley fluid with power law index  $n = n_1$  is identical with that for  $n = n_2 \neq n_1$ . To see this suppose that  $(p^{n_1}, \tau_{ij}^{n_1})$  is the stress tensor for the solution  $\mathbf{u}^{n_1}$  of the problem with  $n = n_1$ , and suppose that  $G^{n_1}(\tau_{ij}^{n_1}) = 0$  for a given  $B$ . Then  $(p^{n_1}, \tau_{ij}^{n_1})$  is admissible for the  $n = n_2$  problem and since  $G^{n_2}(\tau_{ij}^{n_1}) = 0$ , we must also have  $G^{n_2}(\tau_{ij}^{n_2}) = 0$ . Note that the stress fields for the two problems need not be the same. Similarly, we may consider other yield stress

fluid models with analogous Von-Mises yield criteria, such as Casson and Robertson-Stiff fluids. Physically, this just says that until a fluid yields it doesn't *know* if it is a Bingham, Casson or other fluid. It follows also that, for a given  $B$  and bubble shape, if one particular yield stress fluid allows the bubble to propagate, then all do, (i.e., assume otherwise and obtain a contradiction).

A second corollary is as follows. Suppose that  $\Omega_1$  is an enlargement of  $\Omega$ , i.e. we consider the same bubble geometry but in two different sized columns, or we consider a bubble propagating in an infinite media. If the bubble does not propagate in the larger domain, then it will not propagate in the smaller domain. This follows since the stress field for the larger domain can be truncated to the smaller domain and will be admissible, giving a smaller value of  $K_{\bar{\tau}}$ .

### C. Conditions for a bubble to propagate

Using a comparison principle, we can also derive conditions under which a bubble will flow. We have seen that even without a yield stress, surface tension may prevent an appropriately shaped bubble from rising. Therefore, we consider  $\beta = 0$  here. From the results of the previous section, we may consider a Bingham fluid ( $n = 1$ ), i.e., if the bubble propagates in a Bingham fluid, it will do so in any other yield stress fluid (with the same Bingham number). The rate of strain minimization for a Bingham fluid states that  $\mathbf{u}$  is the solution of:

$$\min_{\mathbf{v} \in \bar{V}} J(\mathbf{v}) \equiv \frac{1}{2}a(\mathbf{v}, \mathbf{v}) + j(\mathbf{v}) - L(\mathbf{v}). \quad (61)$$

Similarly, the velocity solution, say  $\mathbf{u}_N$ , for the analogous Newtonian fluid problem, ( $B = 0$ ), satisfies

$$\min_{\mathbf{v} \in \bar{V}} J_N(\mathbf{v}) \equiv \frac{1}{2}a(\mathbf{v}, \mathbf{v}) - L(\mathbf{v}). \quad (62)$$

Note that in the absence of surface tension a bubble will propagate in a Newtonian fluid, and hence  $a(\mathbf{u}_N, \mathbf{u}_N) = L(\mathbf{u}_N) > 0$ .

From (61) & (62):

$$J_N(\mathbf{u}_N) + j(\mathbf{u}_N) = J(\mathbf{u}_N) \geq J(\mathbf{u}). \quad (63)$$

From (35) we have that  $J_N(\mathbf{u}_N) = -\frac{1}{2}a(\mathbf{u}_N, \mathbf{u}_N)$ , and similarly  $J(\mathbf{u}) = -\frac{1}{2}a(\mathbf{u}, \mathbf{u})$ . Therefore we have that:

$$a(\mathbf{u}, \mathbf{u}) \geq a(\mathbf{u}_N, \mathbf{u}_N) - 2j(\mathbf{u}_N), \quad (64)$$

and from the Cauchy-Schwarz inequality  $j(\mathbf{u}_N) \leq B \text{meas}(\Omega)^{1/2} a(\mathbf{u}_N, \mathbf{u}_N)^{1/2}$ . Hence, we have the inequality:

$$a(\mathbf{u}, \mathbf{u}) \geq a(\mathbf{u}_N, \mathbf{u}_N)^{\frac{1}{2}} [a(\mathbf{u}_N, \mathbf{u}_N)^{\frac{1}{2}} - 2B \text{meas}(\Omega)^{\frac{1}{2}}], \quad (65)$$

and the following result.

**Theorem 5:** If  $\mathbf{u}_N$  is the solution to the Newtonian problem for a given bubble, then the bubble will flow in a visco-plastic fluid with Bingham number  $B$ , provided that

$$B < \frac{a(\mathbf{u}_N, \mathbf{u}_N)^{\frac{1}{2}}}{2 \text{meas}(\Omega)^{\frac{1}{2}}}. \quad (66)$$

The proof follows since, under condition (66),  $a(\mathbf{u}, \mathbf{u}) > 0$  for the Bingham fluid, so that  $L(\mathbf{u}) > 0$ . Thus, all other yield stress fluids will flow as well. Theorem 5 may seem a little esoteric. However, if we consider a steadily propagating bubble in a Newtonian fluid, (66) becomes:

$$B < \frac{[V_b U_b]^{\frac{1}{2}}}{2 \text{meas}(\Omega)^{\frac{1}{2}}}, \quad (67)$$

which can be used in an experimental setting, i.e., if a given bubble propagates with speed  $U_b$  in a Newtonian fluid, it will flow in an *equivalently viscous* visco-plastic fluid with yield stress satisfying (67).

## V. EXAMPLES OF BOUNDS

### A. Critical Bingham numbers for a spherical bubble

For a spherical bubble we use the comparison principle, Theorem 4, in order to obtain an estimate of the critical Bingham number. The admissible stress field that we consider is the stress field for the Stokes flow solution around a spherical bubble rising under the influence of gravity in an infinite Newtonian fluid, say  $\tau_{N,ij}$ . We truncate the stress field inside  $\Omega$ .

In terms of a spherical coordinate system  $(r, \theta, \phi)$ , with  $\phi$  being the azimuthal coordinate, (and with the scalings of §II A), the solution is

$$\mathbf{u}_N = (u_N, v_N, w_N) = \left( \frac{\cos \theta}{3r}, -\frac{\sin \theta}{6r}, 0 \right). \quad (68)$$

$$\begin{aligned} \tau_{N,rr} &= -\frac{2 \cos \theta}{3r^2}, & \tau_{N,\theta\theta} &= \frac{\cos \theta}{3r^2}, & \tau_{N,\phi\phi} &= \frac{\cos \theta}{3r^2}, \\ \tau_{N,r\theta} &= 0, & \tau_{N,r\phi} &= 0, & \tau_{N,\theta\phi} &= 0, \\ \Rightarrow \boldsymbol{\tau}_N &= \frac{|\cos \theta|}{\sqrt{3}r^2}, \end{aligned} \quad (69)$$

and finally

$$p_N = p_g - 2\beta + \left[ \frac{1}{3r^2} - r \right] \cos \theta.$$

This solution was first derived by Rybczynski, and independently by Hadamard, in 1911 and can be found in several standard textbooks, e.g., [38, 39]. It can be verified that  $(p_N, \tau_{N,ij})$  satisfy the admissibility conditions, (37)–(40).

The surface of the bubble is at  $r = 1$ , so we find that

$$\boldsymbol{\tau}_N \leq \frac{1}{\sqrt{3}}, \quad \forall \mathbf{x} \in \Omega. \quad (70)$$

Then we may apply Theorem 4, and thus for

$$B \geq K_{\tau_N} = \frac{1}{\sqrt{3}}, \quad (71)$$

the whole fluid region  $\Omega$  is unyielded and the bubble does not move.

A second estimate of the critical Bingham number comes from Theorem 3. We note that for a spherical bubble, the surface tension integral is anti-symmetric and vanishes. this leaves

$$B \geq \frac{1}{2\sqrt{2}}(z_+ - z_-) = \frac{1}{\sqrt{2}}, \quad (72)$$

as our estimate for  $B_c$ . This is clearly more conservative than (71).

## B. Critical Bingham number for long cylindrical bubbles

Here we consider the case of a steadily moving long cylindrical bubble. For our analysis we assume that the bubble is formed of a long cylindrical body with spherical cap ends (see Fig. 5). Furthermore we divide the fluid domain  $\Omega$  into three regions:  $\Omega_3$  is the annular section of fluid within which the bubble has a cylindrical body,  $\Omega_1$  and  $\Omega_2$  are the regions of fluid above and below  $\Omega_3$ , respectively. We derive an approximate bound using (47).

We first note that due to the fore-aft symmetry of the bubble, the surface tension term in (47) vanishes, and we have zero flow provided that:

$$B \geq -\frac{\int_{\Omega} u_3 d\Omega}{\int_{\Omega} \dot{\boldsymbol{\gamma}}(\mathbf{u}) d\Omega}. \quad (73)$$

We make the further simplification that

$$-\frac{\int_{\Omega} u_3 d\Omega}{\int_{\Omega} \dot{\boldsymbol{\gamma}}(\mathbf{u}) d\Omega} \leq -\frac{\int_{\Omega} u_3 d\Omega}{\int_{\Omega_3} \dot{\boldsymbol{\gamma}}(\mathbf{u}) d\Omega},$$

and seek to approximate the bound

$$B \geq -\frac{\int_{\Omega} u_3 d\Omega}{\int_{\Omega_3} \dot{\gamma}(\mathbf{u}) d\Omega}, \quad (74)$$

for which we will also have no flow.

We first consider the numerator of expression (74):  $-\int_{\Omega} u_3 d\Omega$ . We note that

$$-\int_{\Omega} u_3 d\Omega = V_b U_b = \left( \frac{4}{3} \pi r_b^3 + \pi r_b^2 L \right) U_b. \quad (75)$$

From our scaling, we have  $V_b = \frac{4\pi}{3}$ , and hence deduce that for  $L \gg r_b$ :

$$L \sim \frac{4}{3r_b^2}, \quad \text{or} \quad \frac{3r_b^2 L}{4} \sim 1. \quad (76)$$

Hence,

$$-\int_{\Omega} u_3 d\Omega \sim \pi r_b^2 L U_b + O\left(\frac{r_b}{L}\right). \quad (77)$$

To obtain an estimate of  $\int_{\Omega_3} \dot{\gamma}(\mathbf{u}) d\Omega$  we approximate the flow as a one-dimensional axisymmetric flow down the long side of the bubble, i.e., ignoring some small transition region close to each end. The flow in  $\Omega_3$  will have velocity profile similar to that shown schematically in Fig. 6. The only non-zero component of the velocity is in the vertical direction,  $u_3(r)$ . Although we can solve for  $u_3(r)$ , really we are interested only in the limit of zero flow. In this limit, the fluid will only be yielded in a narrow region of thickness  $\alpha$  near the column wall. From mass conservation, the mean velocity in the annular region is  $U_{\text{avg}} = -\frac{\pi r_b^2 U_b}{\pi(R_c^2 - r_b^2)}$ , and this is equal to the unyielded plug velocity, to  $O(\alpha)$ . Thus, in this yielded layer,

$$\dot{\gamma}(\mathbf{u}) = \left| \frac{\partial u_3}{\partial r} \right| \sim \frac{\pi r_b^2 U_b}{\alpha \pi (R_c^2 - r_b^2)},$$

and therefore:

$$\begin{aligned}
\int_{\Omega_3} \dot{\gamma}(\mathbf{u}) d\Omega &\sim \int_0^L \int_0^{2\pi} \int_{R_c-\alpha}^{R_c} r \left| \frac{\partial u_3}{\partial r} \right| dr d\theta dz \\
&\sim \left( \frac{\pi r_b^2 U_b}{\alpha \pi (R_c^2 - r_b^2)} \right) (2\pi \alpha R_c L) \\
&\sim \frac{2\pi r_b^2 R_c L U_b}{R_c^2 - r_b^2}.
\end{aligned} \tag{78}$$

Combining (77) and (78), we see that for  $r_b \ll L$ , our approximate stopping condition becomes:

$$B \gtrsim \frac{1}{2} \frac{R_c^2 - r_b^2}{R_c}, \tag{79}$$

or in terms of  $L$ , using (76):

$$B \gtrsim \frac{1}{2} \frac{R_c^2 - \frac{4}{3L}}{R_c}. \tag{80}$$

### C. A scaling result

As a final bound, we note that we can use the comparison principle of Theorem 4 to derive the following intuitive result. We adopt cylindrical coordinates  $(r, \theta, z)$  for convenience.

**Theorem 6:** Suppose  $\beta = 0$  and we consider an infinite domain  $\Omega$ . If  $r = f(\theta, z)$  denotes a bubble surface which is static for fixed  $B$ , then for  $\lambda < 1$ ,  $r = \lambda f(\theta, z)$  denotes a smaller bubble of the same shape. The flow around this bubble is also static.

The proof is straightforward. We note that if  $\sigma_{ij}$  is the stress tensor for the original ( $\lambda = 1$ ) problem, then for  $\lambda < 1$  we define,  $\tilde{\sigma}_{ij} = \lambda \sigma_{ij}$ . If we also rescale  $\tilde{r} = \lambda r$  and  $\tilde{z} = \lambda z$ , we map the bubble surface onto  $\tilde{r} = \lambda f(\theta, \tilde{z})$ . It may be verified that  $\tilde{\sigma}_{ij}$  is an admissible stress field. Furthermore, since  $\tilde{\tau}_{ij} = \lambda \tau_{ij}$ , it follows that  $\tilde{\tau} < \tau \leq B$ . Therefore, the smaller bubble does not move. The above result also follows simply from the dimensionless scaling we have used.

To incorporate  $\beta > 0$  in Theorem 6 is harder. The result follows from the linearity of the momentum equations, but when we rescale as above, the scaled stress  $\tilde{\sigma}_{nn}$  satisfies an admissibility condition of type (40), but with  $\beta = \lambda^2\beta$ , i.e., so that a smaller bubble with a specific smaller surface tension coefficient will not propagate. Slightly more general results are possible. For example, for a steadily moving axisymmetric bubble with fore-aft symmetry we have seen that the surface tension integrals in the derivation of Theorem 2 disappear and that (40) could be relaxed. For such bubbles, the above scaling result will also hold, i.e. a small bubble will not move if a larger bubble of the same shape does not move.

## VI. DISCUSSION

We have considered the slow propagation of an air bubble in a column of visco-plastic fluid. It was shown that for a given bubble there exists a critical yield stress above which the bubble will not propagate and will remain trapped in the fluid indefinitely. We have obtained a general result for arbitrary bubbles, (47), and a more specific version for steadily moving axisymmetric bubbles, (59). We have also derived a general comparison principle that allows us to use solutions to simpler problems to get additional estimates of the critical yield stress. We have also derived a condition on a maximal Bingham number that can still allow a bubble to propagate.

We have demonstrated our results with some geometrically simple bubble shapes, (a spherical bubble and a long cylindrical bubble), which give some indication of how shape affects the critical yield stress. Additionally, theorem 6 indicates that the intuitive notion that, *if a big bubble does not move, nor will a small one*, is to some extent true.

However, as seen in Fig. 1, static bubbles in yield stress fluids can have a range of

complex shapes. To derive sharp bounds for arbitrary shapes is difficult. In particular we are hampered by two factors. First, the problem appears to be more difficult than that for flow of a visco-plastic fluid around a solid object. For such flows, the yield limits can be approached using boundary layer methods, see e.g. [24]. For a bubble the no slip condition is not satisfied. The location of the *just yielded* boundary layer is then hard to determine. This hampers progress with evaluating the functional in (47). Secondly, in using the comparison principle, e.g. for a Newtonian flow, we have found very few Stokes flow solutions around bubbles, (although there is a well developed theory for axisymmetric solid geometries). Although it is possible, for an axisymmetric bubble, to write out a series expansion of the Newtonian solution, the stress conditions on the bubble surface do not allow simple evaluation of the coefficients.

### **Acknowledgments**

Financial assistance for this research was provided by the Natural Sciences and Engineering Research Council of Canada and the British Columbia Advanced Systems Institute. Their contributions are gratefully acknowledged.

- 
- [1] R. Byron-Bird, G.C. Dai, and B.J. Yarusso. The rheology and flow of viscoplastic materials. *Rev. Chem. Eng.*, 1:2–70, 1983.
  - [2] J.G. Oldroyd. A rational formulation of the equations of motion of a plastic flow for a Bingham solid. *P. Camb. Philos. Soc.*, 43:100–105, 1947.
  - [3] O.L.A. Santos and J.J. Azar. A study of gas migration in stagnant non-newtonian fluids. Technical Report SPE 39019, Society of Petroleum Engineers, 1997.

- [4] A.B. Johnson and D.B. White. Gas rise velocities during kicks. Technical Report SPE 20431, Society of Petroleum Engineers, 1990.
- [5] A. Johnson, I. Rezmer-Cooper, T. Bailey, and D. McCann. Gas migration: Fast, slow or stopped. Technical Report SPE/IADC 29342, Society of Petroleum Engineers, 1995.
- [6] J. Kang, P.B. Butler, and M.R. Baer. A thermochemical analysis of hot spot formation in condensed-phase, energetic materials. *Combust. Flame*, 89:117–139, 1992.
- [7] R. Clift, M.E. Weber, and J.R. Grace. *Bubbles, drops, and particles*. Academic Press, New York, 1978.
- [8] Z. Zapryanov and S. Tabakova. *Dynamics of bubbles, drops and rigid particles*. Fluid Mechanics and its Applications. Kluwer Academic Publishers, Boston, 1999.
- [9] W. Prager. On slow visco-plastic flow. In *Studies in Mathematics and Mechanics*, pages 208–216. Academic Press Inc., New York, 1954. Presented to Richard von Mises by Friends, Colleagues, and Pupils.
- [10] R.R. Huilgol. Variational principles and variational inequalities for a yield stress fluid in the presence of slip. *J. Non-Newtonian Fluid Mech.*, 75:231–251, 1998.
- [11] R.R. Huilgol and Q.D. Nguyen. Variational principles and variational inequalities for the unsteady flows of a yield stress fluid. *Int. J. Non-Linear Mech.*, 36:49–67, 2001.
- [12] R.R. Huilgol. Variational inequalities in the flow of yield stress fluids including inertia: Theory and applications. *Phys. Fluids*, 14(3):1269–1283, 2002.
- [13] K.J. Zwick, P.S. Ayyaswamy, and I.M. Cohen. Variational analysis of the squeezing flow of a yield stress fluid. *J. Non-Newtonian Fluid Mech.*, 63:179–199, 1996.
- [14] I.A. Frigaard, O. Scherzer, and G. Sona. Uniqueness and non-uniqueness in the steady displacement of two visco-plastic fluids. *Z. Angew. Math. Mech.*, 81(2):99–118, 2001.

- [15] I.A. Frigaard, S. Leimgruber, and O Scherzer. Variational methods and maximal residual wall layers. *J. Fluid Mech.*, 483:37–65, 2003.
- [16] I. Frigaard and O. Scherzer. Uniaxial exchange flows of two Bingham fluids in a cylindrical duct. *IMA J. Appl. Math.*, 61:237–266, 1998.
- [17] P.P. Mosolov and V.P. Miasnikov. Variational methods in the theory of the fluidity of a viscous-plastic medium (Variatsionnye metody v teorii techenii viazko-plasticheskoi sredy). *PPM*, 29(3):468–492, 1965.
- [18] P.P. Mosolov and V.P. Miasnikov. On stagnant flow regions of a viscous-plastic medium in pipes (O zastoinykh zonakh techeniia viazko-plasticheskoi sredy v trubakh). *PPM*, 30(4):705–717, 1966.
- [19] P.P. Mosolov and V.P. Miasnikov. On qualitative singularities of the flow of a viscoplastic medium in pipes. *PPM*, 31(3):581–585, 1967.
- [20] G. Duvaut and J.L. Lions. *Inequalities in mechanics and physics*. Springer-Verlag, New York, 1976.
- [21] R. Glowinski. *Numerical methods for nonlinear variational problems*. Springer series in computational physics. Springer-Verlag, New York, 1984.
- [22] S.M. Bhavaraju, R.A. Mashelkar, and H.W. Blanch. Bubble motion and mass transfer in non-Newtonian fluids: Part 1. single bubble in power law and Bingham fluids. *AIChE Journal*, 24(6):1063–1070, 1978.
- [23] S. Stein and H. Buggisch. Rise of pulsating bubbles in fluids with a yield stress. *Z. Angrew. Math. Mech.*, 80(11–12):827–834, 2000.
- [24] A.N. Beris, J.A. Tsamopoulos, R.C. Armstrong, and R.A. Brown. Creeping motion of a sphere through a Bingham plastic. *J. Fluid Mech.*, 158:219–244, 1985.

- [25] J. Blackery and E. Mitsoulis. Creeping motion of a sphere in tubes filled with a Bingham plastic material. *J. Non-Newtonian Fluid Mech.*, 70:59–77, 1997.
- [26] D.D. Atapattu, R.P. Chhabra, and P.H.T. Uhlherr. Creeping sphere motion in Herschel-Bulkley fluids: flow field and drag. *J. Non-Newtonian Fluid Mech.*, 59:245–265, 1995.
- [27] V. Dolejš, P. Doleček, and B. Šiška. Drag and fall velocity of a spherical particle in generalized newtonian and viscoplastic fluids. *Chem. Eng. Process.*, 37:189–195, 1998.
- [28] G Saha, N.K. Purohit, and A.K. Mitra. Spherical particle terminal settling velocity and drag in Bingham liquids. *Int. J. Miner. Process.*, 36:273–281, 1992.
- [29] B.S. Padmavathi, T. Amaranath, and S.D. Nigam. Stokes flow past a sphere with mixed slip-stick boundary conditions. *Fluid Dyn. Res.*, 11:229–234, 1993.
- [30] L. Jossic and A. Magnin. Drag and stability of objects in a yield stress fluid. *AIChE Journal*, 47(12):2666–2672, 2001.
- [31] G. Gheissary and B.H.A.A. van den Brule. Unexpected phenomena observed in particle settling in non-Newtonian media. *J. Non-Newtonian Fluid Mech.*, 67:1–18, 1996.
- [32] I.A. Frigaard. Stratified exchange flows of two Bingham fluids in an inclined slot. *J. Non-Newtonian Fluid Mech.*, 78:61–87, 1998.
- [33] I.A. Frigaard and O. Scherzer. The effects of yield stress variation in uniaxial exchange flows of two Bingham fluids in a pipe. *SIAM J. Appl. Math.*, 60:1950–1976, 2000.
- [34] A.N. Alexandrou and V. Entov. On the steady-state advancement of fingers and bubbles in a Hele-Shaw cell filled by a non-Newtonian fluid. *Euro. J. Appl. Math.*, 8:73–87, 1997.
- [35] M. Allouche, I.A. Frigaard, and G. Sona. Static wall layers in the displacement of two viscoplastic fluids in a plane channel. *J. Fluid Mech.*, 424:243–277, 2000.
- [36] J. Li and Y.Y. Renardy. Shear-induced rupturing of a viscous drop in a Bingham liquid. *J.*

- [37] M.P. do Carmo. *Differential geometry of curves and surfaces*. Prentice Hall, Inc., Englewood Cliffs, NJ, 1976.
- [38] H. Lamb. *Hydrodynamics*. Cambridge University Press, Cambridge, sixth edition, 1975.
- [39] G.K. Batchelor. *An introduction to fluid dynamics*. Cambridge University Press, Cambridge, 1967.

## LIST OF FIGURES:

- Figure 1, Dubash & Frigaard, Physics of Fluids: A variety of interesting static bubble shapes. The bubbles are suspended in a Carbopol solution with a yield stress of approximately 8 Pa. The tubes containing the solution have diameters 25.4mm and 50.8mm.
- Figure 2, Dubash & Frigaard, Physics of Fluids: Physical setup of the problem.
- Figure 3, Dubash & Frigaard, Physics of Fluids: Axisymmetric bubble centred in the column.
- Figure 4, Dubash & Frigaard, Physics of Fluids: Two bubble profiles. The bubble velocities are upwards. For the solid line  $S = -0.010$ , and for the dashed line  $S = 0.012$ .
- Figure 5, Dubash & Frigaard, Physics of Fluids: A long ( $r_b \ll L$ ) cylindrical bubble.
- Figure 6, Dubash & Frigaard, Physics of Fluids: Velocity profile of the flow around the cylindrical section of the bubble.

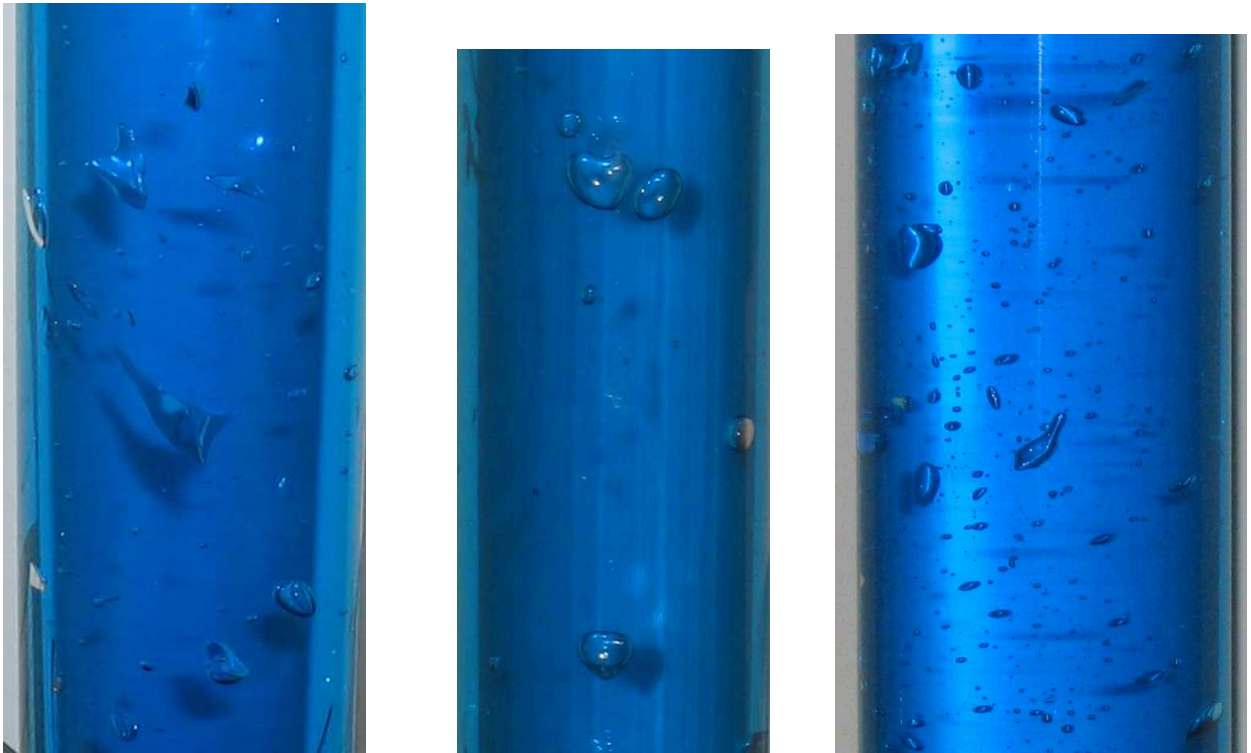


FIG. 1: Dubash & Frigaard, Physics of Fluids: A variety of interesting static bubble shapes. The bubbles are suspended in a Carbopol solution with a yield stress of approximately 8 Pa. The tubes containing the solution have diameters 25.4mm and 50.8mm.

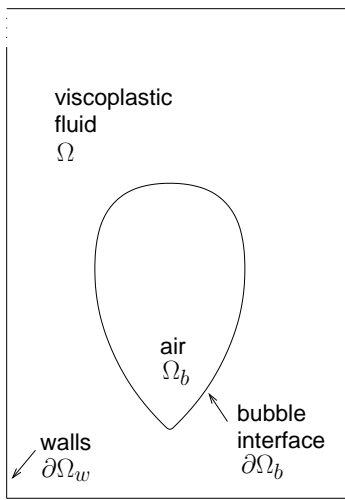


FIG. 2: Dubash & Frigaard, Physics of Fluids: Physical setup of the problem.

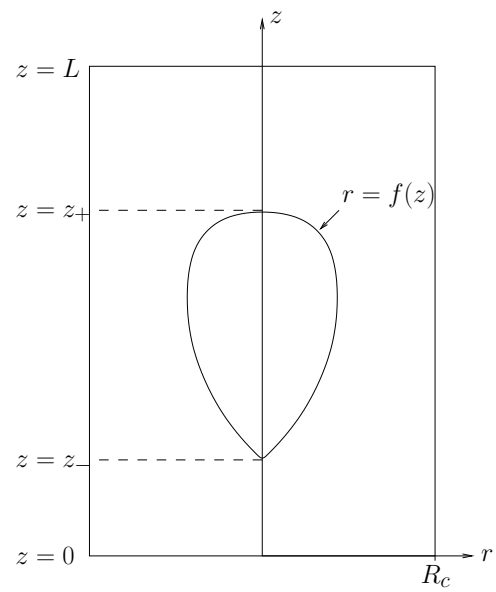


FIG. 3: Dubash & Frigaard, Physics of Fluids: Axisymmetric bubble centred in the column.

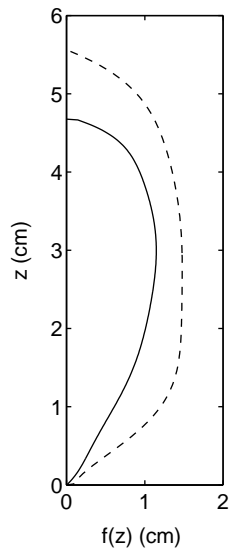


FIG. 4: Dubash & Frigaard, Physics of Fluids: Two bubble profiles. For the solid line  $S = -0.010$ , and for the dashed line  $S = 0.012$ .

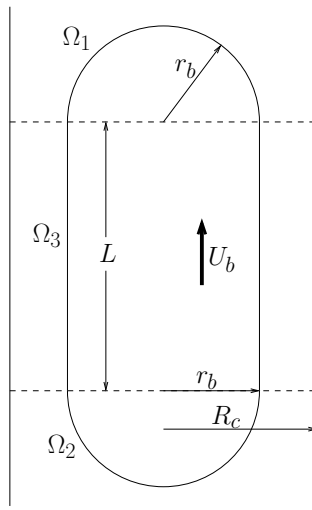


FIG. 5: Dubash & Frigaard, Physics of Fluids: A long ( $r_b \ll L$ ) cylindrical bubble.

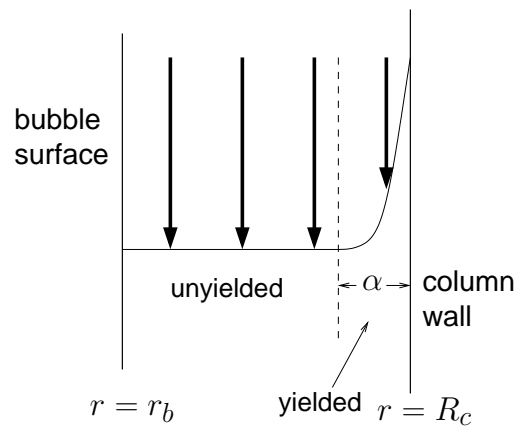


FIG. 6: Dubash & Frigaard, Physics of Fluids: Velocity profile of the flow around the cylindrical section of the bubble.